

Verifying Recurrent Neural Networks using Invariant Inference

Yuval Jacoby¹, Clark Barrett², and Guy Katz¹

¹ The Hebrew University of Jerusalem, Israel
 {yuval.jacoby, g.katz}@mail.huji.ac.il

² Stanford University, USA
 clarkbarrett@stanford.edu

Abstract. Deep neural networks are revolutionizing the way complex systems are developed. However, these automatically-generated networks are opaque to humans, making it difficult to reason about them and guarantee their correctness. Here, we propose a novel approach for verifying properties of a widespread variant of neural networks, called *recurrent neural networks*. Recurrent neural networks play a key role in, e.g., natural language processing, and their verification is crucial for guaranteeing the reliability of many critical systems. Our approach is based on the inference of *invariants*, which allow us to reduce the complex problem of verifying recurrent networks into simpler, non-recurrent problems. Experiments with a proof-of-concept implementation of our approach demonstrate that it performs orders-of-magnitude better than the state of the art.

1 Introduction

The use of *deep neural networks* (DNNs) [19] is on the rise. In recent years, DNNs have successfully been applied in domains such as image classification [35], speaker recognition [25], and game playing [47], often achieving much better performance than hand-crafted software. This trend is likely to continue, and we can already observe first signs of safety-critical systems being designed with DNN components [4, 28].

We focus here on *recurrent neural networks* (RNNs), which are a particular kind of DNNs. Unlike *feed-forward neural networks* (FFNNs), where an evaluation of the network is performed independently of past evaluations, RNNs contain memory units that allow them to retain information from previous evaluations. This renders RNNs particularly suited for tasks that involve context, such as text interpretation. Consider, e.g., the sentence “you only live once, but if you do *it* right, once is enough” (Mae West). In order for a neural network that reads the sentence word-by-word to be able to associate the word *it* with the preceding word *live*, it must retain information about words it had previously encountered. Because of this trait, RNNs are increasingly used in machine translation [11], text summarization [40], health applications [38], speaker recognition [24] and game playing [37].

Part of the success of DNNs is attributed to their very attractive generalization properties: after being trained on a finite set of examples, they generalize well to inputs they have not encountered before [19]. Unfortunately, while this works well on average, it is known that DNNs may react in highly undesirable ways to certain inputs. For instance, it has been observed that many DNNs are vulnerable

to *adversarial attacks* [20], where small, carefully-crafted perturbations are added to an input in order to fool the network into performing significant classification errors. In one recent paper, Cisse et al. [9] proposed an approach for producing such adversarial perturbations that could fool RNNs for automatic speaker recognition. This example, and others, highlight the need to *formally verify* the correctness of RNNs, so that they can be reliably deployed in safety-critical settings. However, while DNN verification has received significant attention in recent years (e.g., [5,13,17,27,31,39,41,50,51,53]), almost all of these efforts have been focused on FFNNs, with very little work done on RNN verification.

To the best of our knowledge, the only existing general approach for RNN verification is via *unrolling* [1]: the RNN is duplicated and concatenated onto itself, creating an equivalent feed-forward network that operates on the sequence of inputs simultaneously, as opposed to one at a time. The FFNN can then be verified using existing FFNN verification technology. The main limitation of this approach is that the transformation greatly increases the network size: if the RNN is to be evaluated over k consecutive inputs, the resulting FFNN is k times larger than the original RNN. Because the complexity of FFNN verification is known to be exponential in network size [29], this reduction gives rise to FFNNs that are difficult to verify — and is hence applicable primarily to small RNNs with short input sequences.

Here, we propose a novel approach for RNN verification, which affords far greater scalability than unrolling. Our approach advocates reducing the RNN verification problem to FFNN verification, but does so in a way that is independent of the number of inputs that the RNN is to be evaluated on, and without duplicating the RNN or otherwise increasing its size. Specifically, our approach consists of two main steps: (i) create an FFNN that *over-approximates* the RNN, but which is the same size as the RNN; and (ii) verify this over-approximation using existing techniques for FFNN verification. In order to perform step (i) we leverage the well-studied notion of *inductive invariants*: our FFNN encodes time-invariant properties of the RNN, which hold initially and continue to hold after the RNN is evaluated on each additional input. Using such invariants allows us to circumvent any duplication of the network or its inputs.

Of course, coming up with meaningful inductive invariants is crucial for the success of this approach. At first we present a general framework that receives the inductive invariants from an oracle, proves that they are indeed invariants, and then uses them in over-approximating the RNN using an FFNN. This semi-automatic framework can be useful, e.g., if a human expert can provide meaningful invariants for the system at hand. Next, in order to render the approach fully automatic, we present an approach for *invariant inference* in RNNs. Automated inference of inductive invariants has been studied extensively in the context of program verification, and is known to be undecidable in general. To mitigate this difficulty, our approach attempts to infer invariants according to predefined *templates*. By instantiating these templates, we automatically generate a candidate invariant I , and then: (i) use our underlying FFNN verification engine to prove that I is indeed an invariant; and (ii) use I in creating the FFNN over-approximation of the RNN, in order to prove the desired property. If either of these steps fail, we refine the invariant I (either strengthening or weakening it, depending on the point of failure), and repeat the process. The process terminates when the property is proven correct, when a counter-example is found, or when a certain timeout value is reached.

In order to evaluate our approach, we created a proof-of-concept implementation in Python. As a feed-forward verification back-end we used the Marabou tool [31] (other engines could also be used). When compared to the state of the art on a set of benchmarks from the domain of speaker recognition [24], our approach performs orders-of-magnitude faster. We intend to make our code and benchmarks publicly available online with the final version of this paper.

To summarize, our contributions are:

1. We propose a general framework for the invariant-based verification of recurrent neural networks. The framework reduces the RNN verification problem to the widely studied FFNN verification problem. The complexity of our procedure is independent of the number of time steps that the RNN is to be evaluated.
2. We propose approaches for automatically inferring invariants for RNNs.
3. We provide an implementation of our technique, as well as a new set of benchmark problems.

The rest of this paper is organized as follows. In Section 2, we provide a brief background on DNNs and their verification. In Section 3, we describe our approach for verifying RNNs via a reduction to FFNN verification, using invariants. We describe automated methods for RNN invariant inference in Section 4, followed by an evaluation of our approach in Section 5. We then discuss related work in Section 6, and conclude with Section 7.

2 Background

2.1 Feed-Forward Neural Networks and their Verification

Feed-forward neural networks (FFNNs) are comprised of an input layer, an output layer, and multiple hidden layers in between. A layer is comprised of multiple nodes (neurons), each connected via edges to nodes from the preceding layer. Each node is assigned a bias value, and each edge is assigned a weight value — both of which are determined when the FFNN is trained. The FFNN is evaluated by assigning values to neurons in the input layer (input neurons), and propagating these values forward through the network (hence the name “feed-forward”). The value of each neuron is computed as a weighted sum of values from the preceding layer, according to the edge weights, plus its bias value. This weighted sum is then passed to a non-linear activation function, and this function’s output becomes the value for the new node.

A simple example appears in Figure 1. The FFNN depicted therein has a single input neuron $v_{1,1}$, a single output neuron $v_{3,1}$, and two hidden neurons $v_{2,1}$ and $v_{2,2}$ in a single hidden layer. All bias values are assumed to be 0. When the input neuron is assigned $v_{1,1} = 4$, the weighted sums for $v_{2,1}$ and $v_{2,2}$ are 4 and -4 , respectively. We use the common $\text{ReLU}(x) = \max(0, x)$ function as our activation function, which yields $v_{2,1} = \text{ReLU}(4) = 4$ and $v_{2,2} = \text{ReLU}(-4) = 0$. Finally, we obtain the output $v_{3,1} = 4$.

More formally, given a DNN N , we use n to denote the number of layers of N . We will use s_i to denote the number of neurons in layer i , also called the *dimension* of layer i . Each hidden layer is associated with a weight matrix W_i of size $s_{i-1} \times s_i$, and a bias vector b_i of size s_i . The DNN input vector will be denoted

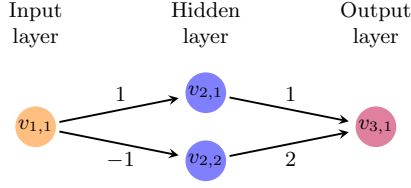


Fig. 1: A simple feed-forward neural network.

as v_1 and the output vector of each hidden layer $1 < i < n$ as $v_i = f(W_i v_{i-1} + b_i)$, where f is some element-wise activation function (such as $\text{ReLU}(x) = \max(0, x)$). The output layer is evaluated similarly, but without an activation function: $v_n = W_{n-1} v_{n-1} + b_n$. We will use $v_{i,j}$ to point to the j 'th neuron in the i 'th layer. Given some input vector v_1 the network then can be evaluated by sequentially calculating v_i for $i = 2, 3, \dots, n$, and v_n will be the output of the network. In the remainder of the paper, we will use x and y to denote the input and output layers, respectively; and $|x|$ to denote the size of the input vector, which is just s_1 . In addition, unless otherwise stated, for simplicity we will assume that all bias values are 0.

Verifying FFNNs. The goal of verifying an FFNN is to establish whether there exist inputs that satisfy certain constraints, such that their corresponding outputs also satisfy certain constraints. Many interesting problems can be cast into this formulation. Looking again at the network from Figure 1, we might wish to know whether it is always the case that $v_{1,1} \leq 5$ entails $v_{3,1} < 20$. Negating the output property, we can use a verification engine to check whether it is possible that $v_{1,1} \leq 5$ and $v_{3,1} \geq 20$. If this query is unsatisfiable (UNSAT), then the original property is bound to hold; but if the query is satisfiable (SAT), as is the case here, then the verification engine will provide us with a counter-example, such as $v_{1,1} = -10, v_{3,1} = 20$.

Formally, we define an FFNN verification query as a triple $\langle P, N, Q \rangle$, where N is an FFNN, P is a predicate over the input variables x , and Q is a predicate over the output variables y . Solving this query entails deciding whether there exists a specific input assignment x_0 such that $P(x_0) \wedge Q(N(x_0))$ holds (where $N(x_0)$ is the output of N for the input x_0). It has been shown that even for simple FFNNs and for predicates P and Q that are conjunctions of linear constraints, the verification problem is NP-complete [29]: in the worst-case, solving it requires a number of operations that is exponential in the number of neurons in N .

2.2 Recurrent Neural Networks

Recurrent Neural Networks (RNNs) are similar to FFNNs, but have an additional construct called a *memory unit*. These memory units are typically introduced for the purpose of modeling data that changes over discrete units of time (time-series data) [15,52]. Memory units achieve this by allowing a hidden neuron to *store* its assigned values for a specific evaluation of the network, and have that value become part of the neuron's weighted sum computation in the *next* evaluation. Thus, when

evaluating the RNN in time step $t + 1$, e.g. when the RNN reads the $t + 1$ 'th word in a sentence, the results of previous evaluations can affect the current result. We say that a DNN is an RNN if at least one of its neurons has a memory unit. An RNN can also contain "regular", memory-less neurons.

A simple example of an RNN appears in Figure 2. There, node $\tilde{v}_{2,1}$ represents node $v_{2,1}$'s memory unit (throughout this paper, we will often draw the memory units as squares, and mark them using the tilde sign). When computing the weighted sum for node $v_{2,1}$, the value of $\tilde{v}_{2,1}$ is also added to the sum, according to its listed weight (1, in this case). Then, once the value of $v_{2,1}$ has been computed, it is stored in $\tilde{v}_{2,1}$ for the next round. In other words, when evaluating $v_{2,1}$ in time step $t + 1$, its value from iteration t is added to the weighted sum; and the final value assigned to $v_{2,1}$ is then stored back in $\tilde{v}_{2,1}$, to be used in iteration $t + 2$. By convention, we assume that all memory units are initialized to 0 for the first evaluation, at time step $t = 1$.

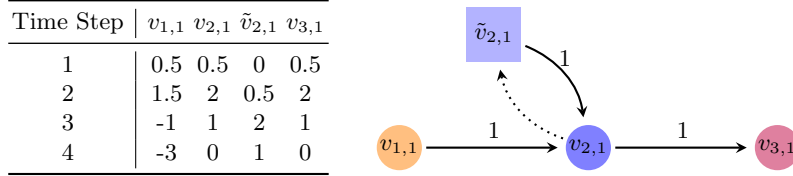


Fig. 2: An illustration of a toy RNN with ReLU activation functions. Each row of the table represents a single time step, and depicts the value of each neuron for that step. Observe that due to the ReLUs functions, the value of $v_{2,1}^t$ is computed as $\max(0, \tilde{v}_{2,1}^{t-1} + v_{1,1}^t)$, where the t superscript represents time step t .

Formally, we define an RNN as follows. We use the same terminology that we did for FFNNs, but add to each node a superscript t to indicate the timestamp of the RNN's evaluation: for example, $v_{3,2}^4$ indicates the value that node $v_{3,2}$ is assigned in the 4'th evaluation of the RNN. Next, we associate each hidden layer of the RNN with a square matrix H_i of dimension s_i , that represents the weights on edges from memory units to neurons. Observe that each memory unit in layer i can contribute to the weighted sums of all neurons in layer i , and not just to the neuron whose values it stores. For time step $t > 0$, the evaluation of each hidden layer $1 < i < n$ is now computed by:

$$v_i^t = f(W_i v_{i-1}^t + H_i v_i^{t-1} + b_i) \quad (1)$$

And by convention, we set v_i^0 to be the zero vector for all layers. The output values are computed by:

$$v_n^t = W_n v_{n-1}^t + H_n v_n^{t-1} + b_n$$

To keep the definition simple, we assume that each hidden neuron in the network has a memory unit. This definition captures also "regular" neurons, by setting the appropriate entries of H to 0, effectively cutting off the memory unit.

For simplicity, in our formulation we focus on activation functions that are applied element-wise. There exist more complex functions, such as Long-Short term Memory (LSTM) [26] or Gated Recurrent Unit (GRU) [7], that are applied to multiple nodes at once. Our technique can be extended to this case, as well; we leave this for future work.

Verifying RNNs. Similarly to the FFNN case, we define an RNN verification query as a tuple $\langle P, N, Q, T_{\max} \rangle$, where P is an input property, Q is an output property, N is an RNN, and $T_{\max} \in \mathbb{N}$ is a bound on the time interval for which the property should hold. P and Q include linear constraints over the network’s inputs and outputs; only now they may also use the notion of time, stipulating, e.g., that output y_2 at the 5’tth time step is at most 10: $y_2^5 \leq 10$.

As a running example, consider the network from Figure 2, denoted by N , the input predicate $P = \bigwedge_{t=1}^5 (-3 \leq v_{1,1}^t \leq 3)$, the output predicate $Q = \bigvee_{t=1}^5 (v_{3,1}^t \geq 16)$, and the time bound $T_{\max} = 5$. This query searches for an evaluation of N with 5 time steps, in which all input values are in the range $[-3, 3]$, and such that at some time step the output value is at least 16. By the weights of N , it can be proved that $v_{3,1}^t$ is at most the sum of the ReLUs of inputs so far, $v_{3,1}^t \leq \sum_{i=1}^t \text{ReLU}(v_{1,1}^i) \leq 3t$; and so $v_{3,1}^t \leq 15$ for all $1 \leq t \leq 5$, and the query is UNSAT.

2.3 Inductive Invariants

Inductive invariants [16] are a well-established way to reason about software with loops. As we later demonstrate, such invariants can be useful in reasoning about RNNs, as these networks perform a loop-like computation.

Formally, let $\langle Q, q_0, T \rangle$ be a transition system, where Q is the set of states, $q_0 \in Q$ is an initial state, and $T \subseteq Q \times Q$ is a transition relation. An invariant I is a logical formula defined over the states of Q , with two properties: (i) I holds for the initial state, i.e. $I(q_0)$ holds; and (ii) I is closed under T , i.e. $(I(q) \wedge \langle q, q' \rangle \in T) \Rightarrow I(q')$. If it can be proved (in a given proof system) that formula I is an invariant, we say that I is an inductive invariant. We use S_I to denote the support of I , i.e. the set $S_I = \{q \in Q \mid I(q)\}$.

Invariants are particularly useful when attempting to verify that a given transition system satisfies a *safety property*. There, we are given a set of bad states B , and seek to prove that none of these states is reachable. We can do so by showing that $S_I \cap B = \emptyset$. Unfortunately, automatically discovering invariants for which the above holds is typically an undecidable problem. Thus, a common approach is to restrict the search space — i.e., to only search for invariants with a certain syntactic form. As we later discuss, in the context of RNNs such an approach is often sufficient for coming up with useful inductive invariants.

3 Reducing RNN Verification to FFNN Verification

3.1 Unrolling

To date, the only available general approach for verifying RNNs [1] is to transform the RNN in question into a *completely equivalent*, feed-forward network, using *unrolling*. An example appears in Figure 3. The idea is to leverage T_{\max} , which is an upper bound on the number of times that the RNN will be evaluated. The RNN is duplicated T_{\max} times, once for each time step in question, and its memory units are removed. Finally, the nodes in the i ’th copy are used to fill the role of memory units for the $i + 1$ ’th copy of the network.

While unrolling gives a sound reduction from RNN verification to FFNN verification, it unfortunately tends to produce very large networks. When verifying a

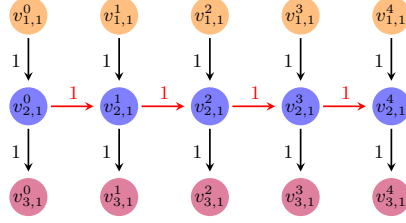


Fig. 3: Unrolling of the network from Figure 2, for $T_{\max} = 5$ time units. The edges in red fill the role of the memory units of the original RNN. The number of neurons in the unrolled network is 5 times the number of neurons in the original.

property that involves t time steps, an RNN network with n memory units will be transformed into an FFNN with $(t - 1) \cdot n$ new nodes. Because the FFNN verification problem becomes exponentially more difficult as the network size increases [29], this renders the problem infeasible for large values of t . As scalability is a major limitation of existing FFNN verification technology, unrolling can currently only be applied to small networks that are evaluated for a small number of time steps.

3.2 Circumventing Unrolling

We propose a novel alternative to unrolling, which can reduce RNN verification to FFNN verification without the blowup in network size. The idea is to transform a verification query $\varphi = \langle P, N, Q, T_{\max} \rangle$ over an RNN N into a different verification query $\hat{\varphi} = \langle \hat{P}, \hat{N}, \hat{Q} \rangle$ over an FFNN \hat{N} . $\hat{\varphi}$ is not equivalent to φ , but rather *over-approximates* it. The approximation is constructed in a way that guarantees that if $\hat{\varphi}$ is UNSAT, then φ is also UNSAT. In other words, if the modified property holds for \hat{N} , then the original property holds for N . As is often the case, if $\hat{\varphi}$ is SAT, either the original property truly does not hold for N , or the invariant I was *too weak*. In the latter case, we can strengthen I and try again; we discuss this case later.

A key point in our approach is that $\hat{\varphi}$ is created in a way that captures the notion of time in the FFNN setting, and without increasing the network size. This is done by incorporating into \hat{P} an *invariant*, that puts bounds on the memory units as a function of the time step t . This invariant does not precisely compute the values of the memory units — instead, it bounds each of them in an interval. This inaccuracy is what makes $\hat{\varphi}$ an over-approximation of φ . More specifically, the construction is performed as follows:

1. \hat{N} is constructed from N by adding a new input neuron, t , to represent time. Because FFNNs typically deal with continuous inputs, we will treat t as a real number.
2. For every node v with memory unit \tilde{v} , in \hat{N} we *replace* \tilde{v} with a regular neuron, v^m , which is placed in the input layer. The m superscript signifies that this neuron replaces a memory unit. Neuron v^m will be connected to the network's original neurons, just as \tilde{v} was, and with the same weights as before.³

³ Note that we slightly abuse the definitions from Section 2, by allowing an input neuron to be connected to neurons in layers other than its preceding layer.

3. We set $\hat{P} = P \wedge (1 \leq t \leq T_{\max}) \wedge I$, where I is a formula that bounds the values of each new v^m node as a function of the time step t . The constraints in I constitute the invariant over the memory units' values.
4. The output property is unchanged: $\hat{Q} = Q$.

We name $\hat{\varphi}$ and \hat{N} constructed in this way the *snapshot query* and the *snapshot network*, respectively, and denote $\hat{\varphi} = \mathcal{S}(\varphi)$ and $\hat{N} = \mathcal{S}(N)$. The intuition behind this construction is that query $\hat{\varphi}$ encodes a snapshot (an assignment of t) in which all constraints are satisfied. At this point in time, the v^m nodes represent the values stored in the memory units (whose assignments are bounded by the invariant I); and the input and output nodes represent the network's inputs and outputs at time t . Clearly, a satisfying assignment for $\hat{\varphi}$ does not necessarily indicate a counter-example for φ ; e.g., because the values assigned to v^m might be impossible to obtain at time t in the original network. However, if $\hat{\varphi}$ is UNSAT then so is φ , because there does not exist a point in time in which the query might be satisfied. Note that the construction only increases the network size by 1 (the v^m neurons replace the memory units, and we add a single neuron t).

Time-Agnostic Properties. In the aforementioned construction of $\hat{\varphi}$, the original properties P and Q appear, either fully or as a conjunct, in the new properties \hat{P} and \hat{Q} . It is not immediately clear that this is possible, as P and Q might also involve time. For example, if P is the formula $v_{1,2}^7 \geq 10$, it cannot be directly incorporated into \hat{P} , because \hat{N} has no notion of time step 7.

To overcome this difficulty, we make the following simplifying assumption: we assume that P and Q are time-agnostic, and are given in the following form: $P = \bigwedge_{t=1}^{T_{\max}} \psi_1$ and $Q = \bigvee_{t=1}^{T_{\max}} \psi_2$, where ψ_1 and ψ_2 are formulas that include linear constraints over the inputs and outputs of N , respectively, at time stamp t . This formulation can express queries in which the inputs are always in a certain interval, and a bound violation of the output nodes is sought. Our running example from Figure 2 fits this form. When the properties are given in this form, we set $\hat{P} = \psi_1$ and $\hat{Q} = \psi_2$, with the t superscripts omitted for all neurons. Later, in Section 4.4, we relax this limitation significantly.

Example. In Figure 4 we demonstrate our approach on the running example from Figure 2. Recall that in that example, our constraints were $P = \bigwedge_{t=1}^5 (-3 \leq v_{1,1}^t \leq 3)$, and $Q = \bigvee_{t=1}^5 (v_{3,1}^t \geq 16)$. First, we add a new input neuron, marked t , to represent the time step. Next, we replace the memory unit $\tilde{v}_{2,1}$ with a regular neuron, $v_{2,1}^m$. Node $v_{2,1}^m$ is connected to node $v_{2,1}$ with weight 1 (the same weight previously found on the edge from $\tilde{v}_{2,1}$ to $v_{2,1}$). Next, we set \hat{P} to be the conjunction of (i) P , with its internal conjunction and t superscripts omitted; (ii) the time constraint $1 \leq t \leq 5$; and (iii) the invariant that bounds the values of $v_{2,1}^m$ as a function of time: $v_{2,1}^m \leq 3(t-1)$. Our new verification query is thus:

$$\underbrace{\langle (-3 \leq v_{1,1} \leq 3) \wedge (1 \leq t \leq 5) \wedge (v_{2,1}^m \leq 3(t-1)) \rangle}_{\hat{P}}, \underbrace{\langle \hat{N}, v_{3,1} \geq 16 \rangle}_{\hat{Q}}$$

where \hat{N} is the network in Figure 4. This query is, of course, UNSAT, indicating that the original query is also UNSAT. Note that the new node t is not connected

to any other node; it is added solely for the purpose of including it in constraints that appear in \hat{P} .

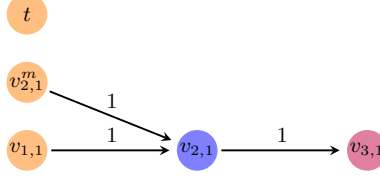


Fig. 4: The feed-forward snapshot network \hat{N} for the RNN from Figure 2. We introduce two new nodes: t to represent the time step, and $v_{2,1}^m$ to take over the role of the memory unit $\tilde{v}_{2,1}$.

The requirement that I be an invariant over the memory units of N ensures that our approach is sound. Specifically, it guarantees that I allows any assignment for v^m that the original memory unit \tilde{v} might be assigned. For instance, looking at the example from Figure 2, consider the input sequence $v_{1,1}^1 = 2, v_{1,1}^2 = -1, v_{1,1}^3 = 3$. This sequence implies that at the beginning of the fourth evaluation, $\tilde{v}_{2,1}^4 = v_{2,1}^3 = 2 - 1 + 3 = 4$. Our invariant I , which states that $v_{2,1}^m \leq 3(t-1)$ allows this, because $4 < 3 \cdot 3 = 9$. On the other hand, $I' = (v_{2,1}^m \leq t-1)$ is not a valid invariant for this example, because it forbids a possible assignment of $v_{2,1}^m$.

The soundness guarantee is formulated in the following lemma (whose proof, by induction, is straightforward and is omitted due to lack of space):

Lemma 1. *Let $\varphi = \langle P, N, Q, T_{\max} \rangle$ be an RNN verification query, and let $\hat{\varphi} = \langle \hat{P}, \hat{N}, \hat{Q} \rangle$ be the snapshot query $\hat{\varphi} = \mathcal{S}(\varphi)$. Specifically, let \hat{N} be constructed from N by adding a time neuron t and by replacing each memory unit \tilde{v} with an input neuron v^m ; and let $\hat{P} = P \wedge (1 \leq t \leq T_{\max}) \wedge I$. If I is an invariant that bounds the values of each v^m , and if $\hat{\varphi}$ is UNSAT, then φ is also UNSAT.*

3.3 Constructing $\hat{\varphi}$: Verifying the Invariant

In Section 3.2 we described a reduction from RNN verification to FFNN verification. A key assumption was that the oracle-provided formula I , which bounds the memory units as a function of the time t , was truly an invariant. This assumption is risky, as a malicious (or simply mistaken) oracle could provide a bogus invariant, jeopardizing the soundness of the process as a whole. In this section we make our method more robust, by including a step that verifies that I is indeed an invariant. This step, too, is performed by creating an FFNN verification query, which can then be dispatched using the back-end FFNN verification engine.

In Section 2.3 we defined the notion of an inductive invariant. In the context of an RNN N , we define the state space Q as the set of states $q = \langle \mathcal{A}, t \rangle$ where \mathcal{A} is the current assignment to the nodes of N (including the assignments of the memory units), and t is a natural number representing the time step. For another state $q' = \langle \mathcal{A}', t' \rangle$, the transition relation $T(q, q')$ holds if and only if:

1. $t' = t + 1$; i.e., the time step has advanced by one;

2. for each memory unit \tilde{v} associated with neuron v , it holds that $\mathcal{A}'[\tilde{v}] = \mathcal{A}[v]$; i.e., the assignment of each neuron in \mathcal{A} is stored in its corresponding memory unit in \mathcal{A}' ; and
3. the assignment \mathcal{A}' of all of the network's neurons constitutes a proper evaluation of the RNN according to Section 2; i.e., all weighted sums and activation functions are computed properly.

A state q_0 is initial if the time step is 1, all memory units are assigned to 0, and the assignment of all of the network's neurons constitutes a proper evaluation of the RNN (there may be multiple initial states).

Next, let I be a formula over the memory units of N , and suppose we wish to verify that I is an invariant. We slightly abuse notation, and treat I as a formula over both the RNN N and its snapshot network $\hat{N} = \mathcal{S}(N)$; for the latter, every occurrence of memory unit \tilde{v}^t is renamed to v^m . Proving that I is invariant amounts to proving that $I(q_0)$ holds for any initial state q_0 , and that for every two states $q, q' \in Q$, if $I(q)$ then also $I(q')$. Checking whether $I(q_0)$ holds is trivial: in the initial step, all memory units are set to 0, and we can easily check that I holds for this assignment. The second check is more tricky; here, the key point is that because q and q' are consecutive states, the memory units of q' are simply the neurons of q . Thus, we can prove that I holds for q' by looking at the snapshot network, assuming that I holds initially, and proving that $I[v^m \mapsto v, t \mapsto t+1]$, i.e. the invariant with each memory unit v^m renamed to its corresponding neuron v and the time step advanced by 1, also holds. The resulting verification query, which we term φ_I , can be verified using the underlying FFNN verification back-end.

We use our running example from Figure 2 to illustrate this process. Let $I = v_{2,1}^m \leq 3(t-1)$ be our candidate invariant. We begin by checking that I holds at every initial state q_0 ; this is true because at time $t = 1$, $v_{2,1}^m = 0 \leq 3 \cdot 0$. Next, we assume that I holds for state $q = \langle \mathcal{A}, t \rangle$ and prove that it holds for $q = \langle \mathcal{A}', t+1 \rangle$. First, we create the snapshot FFNN \hat{N} , shown in Figure 4. We then extend the original input property $P = \bigwedge_{t=1}^5 (-3 \leq v_{1,1}^t \leq 3)$ into a property P' that also captures our assumption that the invariant holds at time t :

$$P' = (-3 \leq v_{1,1} \leq 3) \wedge (v_{2,1}^m \leq 3(t-1)).$$

Finally, we prepare an output property Q' that asserts that the invariant does not hold for $v_{2,1}$ at time $t+1$, by renaming $v_{2,1}^m$ to $v_{2,1}$ and incrementing t :

$$Q' = \neg(v_{2,1} \leq 3(t+1-1)).$$

When the FFNN verification engine answers that $\varphi_I = \langle P', \mathcal{S}(N), Q' \rangle$ is **UNSAT**, we can conclude that I is indeed an invariant. In cases where the query turns out to be **SAT**, I is not an invariant, and the counter-example returned by the underlying verifier can be used to refine it.

The steps described in this section, namely (i) prove that a formula I is an invariant; (ii) use I to create a query $\hat{\varphi}$ that over-approximates the original query φ ; and (iii) prove that $\hat{\varphi}$ is **UNSAT**, allow us to automatically reduce the RNN verification problem to the FFNN verification problem. The only part of the process that is not automated is coming up with the invariant I — which is the topic of the following section.

4 Invariant Inference

In order to reduce RNN verification to FFNN verification, we require an invariant I that bounds the values of each memory unit as a function of time t . In general, automatically discovering such invariants is an undecidable problem [44]. To mitigate this difficulty we restrict ourselves to invariants that follow a *linear template*.

4.1 Single Memory Unit

We begin with a simple case, in which the network has a single hidden node v with a memory unit (we will relax this limitation later). Note that this is the case in the running example depicted in Figure 2. Here, inferring an invariant according to a linear template means finding values α_l and α_u , such that:

$$\alpha_l \cdot (t - 1) \leq \tilde{v}^t \leq \alpha_u \cdot (t - 1) \quad (2)$$

Thus, the goal is to bound the value of \tilde{v}^t from below (using α_l) and from above (using α_u), both as a function of time. For simplicity, we focus only on finding the upper bound; the lower bound case is symmetrical. For our running example, we have already seen such an upper bound, which was sufficiently strong for proving the desired property: $\tilde{v}_{2,1}^t \leq 3(t - 1)$.

Once candidate α 's are proposed, verifying that the invariant holds can be performed using the techniques outlined in Section 3. There are two places where the process might fail: (i) the proposed invariant cannot be proved (φ_I is **SAT**), because a counter-example exists. This means that our invariant is *too strong*, i.e. the bound is too tight. In this case we can weaken the invariant by increasing α_u ; or (ii) the proposed invariant holds, but the FFNN verification problem that it leads to, $\hat{\varphi}$, is **SAT**. In this case, the invariant is *too weak*; it is indeed an invariant, but does not imply the desired output property. In this case, we can strengthen the invariant by decreasing α_u .

To illustrate these possible failures, we return to our running example from Figure 2. Assume we set $\alpha_u = 100$. This value gives rise to a valid upper bound (since we know that $\tilde{v}_{2,1}^t \leq 3(t - 1) \leq 100t$). However, this invariant is too weak to prove that $\hat{\varphi}$ is **UNSAT**; for example, assigning $t = 4$, $v_{1,1} = 0$ and $v_{2,1}^m = 40$ will imply $v_{3,1} = 40$ which satisfies the output condition $Q = \bigvee_{t=1}^5 (v_{3,1}^t \geq 16)$. We can conclude that a stronger invariant, i.e. a smaller α_u , is required. For the other possible failure, let us set $\alpha_u = 1$; in this case, the resulting formula is not an invariant, e.g. because of the input assignment $v_{1,1} = 3$, $t = 1$ and $v_{2,1}^m = 0$, which leads to $v_{2,1} = 3 > 1 \cdot (t + 1)$. This implies that a greater α_u is required.

The aforementioned example leads us to binary search strategy. We define a search range $[lb, ub]$ for α_u . Initially, $lb = -M$ and $b = M$ for a very large constant M . We set $\alpha = \frac{1}{2}(lb + ub)$, and attempt our procedure. If the candidate invariant is too weak, ub is decreased; and if it is too strong, lb is increased. The search stops, i.e. an optimal invariant is found, when $ub - lb \leq \epsilon$ for a small constant ϵ . The result verification procedure (for networks with a single memory unit) is described in Alg. 1. The algorithm fails if the optimal linear invariant is found, but is insufficient for proving the property in question; this can happen if φ is indeed **SAT**, or if a more sophisticated invariant is required. The algorithm can be extended in a straightforward manner to incorporate lower bound invariants as well.

Algorithm 1 Automatic Single Memory Unit Verification(P, N, Q, T_{\max})

```
1:  $lb \leftarrow -M, ub \leftarrow M$  ▷  $M$  is a large constant
2: while  $ub - lb \geq \epsilon$  do
3:    $\alpha_u \leftarrow \frac{ub+lb}{2}$ 
4:    $I \leftarrow v_{2,1}^m \leq \alpha_u \cdot t$ 
5:   if  $\varphi_I$  is UNSAT then
6:     Construct  $\hat{\varphi}$  using invariant  $I$ 
7:     if  $\hat{\varphi}$  is UNSAT then
8:       return True
9:      $ub \leftarrow \alpha_u$  ▷ Invariant too weak
10:  else
11:     $lb \leftarrow \alpha_u$  ▷ Invariant too strong
12: return False
```

Linear Templates: Pros and Cons. Using linear invariant templates affords two key benefits. First, the generated invariants have a simple form, and approaches based on binary-search can be used to optimize them. Second, because linear constraints can be encoded into most FFNN verification tools, the resulting φ_I queries can be verified automatically; this would not have been the case, e.g., if we had used upper bounds that are quadratic in t , which FFNN verification tools typically do not support. The downside of using the linear template is that we might miss out on more complex invariants, which may be required to prove the property at hand. Identifying additional kinds of templates that are both expressive and supported by FFNN verification tools is an important avenue for future work.

4.2 Multiple Layers with Single Memory Units

We now extend our approach from RNNs with a single memory unit to RNNs with multiple memory units, each in a separate layer. The extension is performed in an iterative fashion. As before, we begin by constructing the snapshot network in which all memory units are replaced by regular neurons. Next, we work layer by layer and generate invariants that over-approximate each memory unit. As we go into deeper layers of the network, we use previously-proven invariants in order to bound the current memory unit. Eventually, all memory units are over-approximated using invariants, and we can attempt to prove the desired property.

An example appears in Figure 5. Let $P = \bigwedge_{t=1}^5 (-3 \leq v_{1,1}^t \leq 3)$ and $Q = \bigvee_{t=1}^5 (v_{4,1}^t \geq 60)$. First we construct the snapshot network shown in the figure. Next, we prove the invariant $v_{2,1}^m \leq 3(t-1)$, same as we did before. This invariant bounds the values of $v_{2,1}^m$. Next, we use this information in proving an invariant also for $v_{3,1}$; e.g., $v_{3,1}^m \leq 9 \cdot (t-1)$. To see why this is an invariant, observe that

$$v_{3,1}^t = \sum_{i=1}^t v_{2,1}^i \leq \sum_{i=1}^t 3i = (3+3t) \frac{t}{2} \leq (3+3T_{\max}) \frac{t}{2} = 9t$$

Note that the invariant for $v_{2,1}$ was used in the $*$ transition. Once this invariant is proved, we can show that the original property holds, by using FFNN verification

to show that the following snapshot query in UNSAT:

$$\langle (-3 \leq v_{1,1} \leq 3) \wedge (1 \leq t \leq 5) \wedge (v_{2,1}^m \leq 3(t-1)) \wedge (v_{3,1}^m \leq 9(t-1)), \mathcal{S}(N), v_{4,1} \geq 60 \rangle$$

where $\mathcal{S}(N)$ is the FFNN from Figure 5.

The general algorithm for this case is given as Alg. 2. We assume for simplicity that *every* hidden layer in the RNN has a (single) memory unit. Initially (Lines 2-5), the algorithm guesses and verifies a very coarse upper bound on each of the memory units. Next, it repeatedly attempts to solve the snapshot query $\hat{\varphi}$ using the current invariants. If successful, we are done (Line 9); and otherwise, we start another pass over the network’s layers, attempting to strengthen each invariant in turn. We know we have reached an optimal invariant for a layer when the search range for that layer’s α becomes smaller than some small ϵ constant (Line 13). The algorithm fails (Line 22) when (i) optimal invariants for all layers have been discovered; and (ii) these optimal invariants are insufficient for solving the snapshot query. As before, the algorithm only deals with upper bounds, and can be extended to incorporate lower bound invariants as well.

Algorithm 2 Automatic Multiple Memory Units Verification(P, N, Q, T_{\max})

```

1: Construct the snapshot network  $\hat{N}$ 
2: for  $i = 2$  to  $n - 1$  do
3:    $lb_i \leftarrow -M, ub_i \leftarrow M, \alpha_i \leftarrow M$  ▷  $M$  is a large constant
4:    $I_i \leftarrow v_i^m \leq \alpha_i \cdot t$  ▷ Loose invariant, should hold
5:   if  $\varphi_{I_i}$  is SAT then return False ▷ Loose invariant fails, give up
6: while True do
7:   Construct  $\hat{\varphi}$  using the invariant  $\bigwedge_{i=2}^{n-1} I_i$ 
8:   if  $\hat{\varphi}$  is UNSAT then
9:     return True ▷ Invariants sufficiently strong
10:  else
11:    progressMade  $\leftarrow$  False
12:    for  $i = 2$  to  $n - 1$  do
13:      if  $ub_i - lb_i \leq \epsilon$  then ▷ Already have optimal invariant
14:        Continue ▷ Still searching for optimal invariant
15:      progressMade  $\leftarrow$  True
16:       $\alpha'_i \leftarrow (ub_i + lb_i)/2$ 
17:       $I'_i \leftarrow v_i^m \leq \alpha'_i \cdot t$ 
18:      if  $\varphi_{I'_i}$  is UNSAT then
19:         $I_i \leftarrow I'_i, \alpha_i \leftarrow \alpha'_i, ub_i \leftarrow \alpha_i$  ▷ Better invariant found
20:      else
21:         $lb_i \leftarrow \alpha'_i$  ▷ Invariant unchanged, range shrinks
22:      if !progressMade then return False ▷ Best invariants too weak

```

4.3 Layers with Multiple Memory Units

We now extend our approach to support the most general case: an RNN with layers that contain multiple memory units. The idea is the same as in Alg. 2: we iteratively infer and prove invariants for each layer, leveraging the already-proven invariants from layer k when proving invariants for layer $k + 1$. Once all layers have

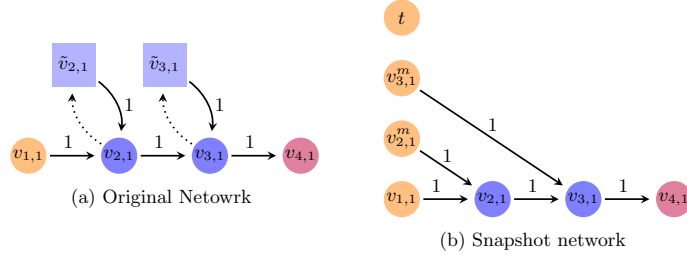


Fig. 5: An RNN with multiple memory units, in separate layers (on the left), and its snapshot network (on the right).

been handled, we attempt to show that the snapshot query is **UNSAT**; and if that fails, we go back and strengthen previous invariants.

The main difficulty is in inferring invariants for a layer that has multiple memory units. Figure 6 depicts a simple example of an RNN that has a single layer with multiple memory units (although the technique applies also to RNNs with multiple layers with memory units). The key point is that while each memory unit belongs to a single neuron, it affects the assignments of all other neurons in that layer.

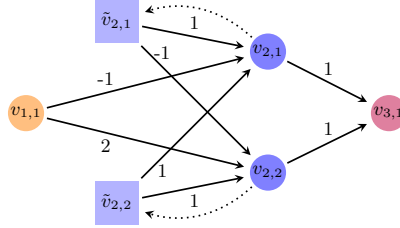


Fig. 6: An RNN with a 2-dimensional recurrent layer. Both memory units affect both neurons of the hidden layer: $v_{2,1}^t = \text{ReLU}(\tilde{v}_{2,1}^t + \tilde{v}_{2,2}^t - v_{1,1}^t)$; and $v_{2,2}^t = \text{ReLU}(-\tilde{v}_{2,1}^t + \tilde{v}_{2,2}^t + 2v_{1,1}^t)$.

We propose to handle this case using separate linear invariants for upper- and lower-bounding each of the memory units. However, while the invariants have the same linear form as in the single memory unit case, *proving* them requires taking the other invariants of the same layer into account. Consider the example in Figure 6, and suppose we have α_l^1, α_u^1 and α_l^2, α_u^2 for which we wish to verify that

$$\alpha_l^1 \cdot t \leq v_{2,1}^t \leq \alpha_u^1 \cdot t \quad \alpha_l^2 \cdot t \leq v_{2,2}^t \leq \alpha_u^2 \cdot t \quad (3)$$

In order to prove these bounds we need to dispatch an FFNN verification query that assumes Eq. 3 holds and uses it to prove the inductive step:

$$v_{2,1}^{t+1} = \text{ReLU}(-v_{1,1}^t + v_{2,1}^t + v_{2,2}^t) \leq \alpha_u^1 \cdot (t+1) \quad (4)$$

Similar steps must be performed for $v_{2,1}^{t+1}$'s lower bound, and also for $v_{2,2}^{t+1}$'s lower and upper bounds. The key point is that because Eq. 4 involves $v_{2,2}^t$, the bounds proved for this neuron, and hence the values of α_l^2 and α_u^2 , must be used. In the

single memory unit case, whenever Eq. 4 did not hold we would increase the value of α ; and if proving the desired property failed, we would decrease the value of α . Here, the situation is more complex; specifically, it is possible that increasing α_1^u would invalidate previously acceptable assignments for α_l^2 or α_u^2 .

For example, consider the network in Figure 6, with $P = \bigwedge_{t=1}^3 -3 \leq v_{1,1}^t \leq 3$, and $Q = \bigvee_{t=1}^3 v_{3,1}^t \geq 90$. Our goal is to find values for α_l^1, α_u^1 and α_l^2, α_u^2 that will satisfy Eq. 3. Let us consider $\alpha_l^1 = 0, \alpha_u^1 = 5, \alpha_l^2 = 0$ and $\alpha_u^2 = 0$. Using these values, the induction hypothesis (Eq. 3) and the bounds for $v_{1,1}$, we can indeed prove the upper bound for $v_{2,1}^t$:

$$v_{2,1}^{t+1} = \text{ReLU}(-v_{1,1}^t + v_{2,1}^t + v_{2,2}^t) \leq -v_{1,1}^t + v_{2,1}^t + v_{2,2}^t \leq 3 + 5t + 0 \leq 5(t+1)$$

Unfortunately, the bounds $0 \leq v_{2,2}^t \leq 0$ are inadequate, because $v_{2,2}^t$ can take on positive values. We are thus required to adjust the α values, for example by increasing α_u^2 to 2. However, this change invalidates the upper bound for $v_{2,1}^t$, i.e. $v_{2,1}^t \leq 5t$, as that bound relied on the upper bound for $v_{2,2}^t$; specifically, knowing only that $-3 \leq v_{1,1}^t \leq 3$, $0 \leq v_{2,1}^t \leq 5t$ and $0 \leq v_{2,2}^t \leq 2t$, it is impossible to show that $v_{2,1}^{t+1} \leq 5(t+1)$. Next, trying the assignment $\alpha_l^1 = 0, \alpha_u^1 = 25, \alpha_l^2 = 0$ and $\alpha_u^2 = 6$, the resulting invariants are provable. Unfortunately, these invariants are insufficient for solving the snapshot query, i.e. to show that $v_{3,1}^t < 90$; to see this, recall that $v_{3,1}^t = v_{2,1}^t + v_{2,2}^t$, and thus the strongest bound we can show is $v_{3,1}^t \leq v_{2,1}^t + v_{2,2}^t = 25t + 6t$, which does not imply $v_{3,1}^t < 90$ for $T_{\max} = 3$. Thus, our invariants need to be strengthened — by either increasing α_l^1 or α_l^2 , or by decreasing α_u^1 or α_u^2 . We observe that adjusting α_u^1 to 21 produces a valid set of invariants that imply the unsatisfiability of the snapshot query.

The example above demonstrates the intricate dependencies between the α values, and the complexity that these dependencies add to the search process. Unlike in the single memory unit case, it is not immediately clear how to find an initial invariant that simultaneously holds for all memory units, or how to strengthen this invariant (e.g., which α constant to try and improve).

Finding an Initial Invariant. We propose to encode the problem of finding initial α values as a *mixed integer linear program* (MILP) [8]. The constraints that the α values must satisfy (e.g., Eq. 4) include weighted sums and piecewise-linear activation functions. Weighted sums can be encoded directly in MILP, and the piecewise-linear constraints can also be encoded in a straightforward way, using big-M encoding [2,29]. There are two main advantages to using MILP in this context:

- assuming only piecewise-linear activation functions, the problem can be precisely encoded in MILP. This means that the MILP solver is guaranteed to return a valid invariant, or soundly report that no such invariant exists.
- MILP instances also include a *cost function* to be minimized. We can leverage this fact to optimize our starting invariant; for example, by setting the cost function to be $\sum \alpha_u - \sum \alpha_l$, the MILP solver will typically suggest a solution in which the upper bound α 's are small and the lower bound α 's are large.

The main disadvantage to using MILP is that, in order to ensure that the invariants hold for all time steps $1 \leq t \leq T_{\max}$, we must encode all of these steps in the MILP query. For example, going back to Eq. 4, in order to guarantee that

$$v_{2,1}^{t+1} = \text{ReLU}(-v_{1,1}^t + v_{2,1}^t + v_{2,2}^t) \leq \alpha_u^1 \cdot (t+1)$$

we would need to encode within our MILP instance the fact that

$$\bigwedge_{t=1}^{T_{\max}} (\text{ReLU}(-v_{1,1}^t + v_{2,1}^t + v_{2,2}^t) \leq \alpha_u^1 \cdot (t+1))$$

which might render the MILP instance difficult to solve for large values of T_{\max} .

MILP solvers are mature tools, and can handle very large input instances; and indeed, in our experiments, this was never the bottleneck. Still, should this become a problem, we propose to encode only a subset of the values of $t \in \{1, \dots, T_{\max}\}$, making the problem easier to solve; and should the α assignment fail to produce an invariant (this will be discovered when φ_I is verified), additional constraints can be added to guide the MILP solver towards a correct solution.

Strengthening the Invariant. If we are unable to prove that snapshot query $\hat{\varphi}$ is UNSAT for a given I , then the invariant needs to be strengthened. We propose to achieve this by invoking the MILP solver again, this time adding new linear constraints that force the selection of tighter bounds. For example, if the current invariant is $\alpha_l = 3, \alpha_u = 7$, we propose to add constraints specifying that $\alpha_l \geq 3 + \epsilon$ and $\alpha_u \leq 7 - \epsilon$, for some small positive ϵ . This guarantees a strengthening of the invariants, although the improvement may be very small — depending on the value of ϵ being used. It is possible to require the strengthening of all α values, or to stipulate this only for some of the values, based on some heuristics.

Invariants without using MILP. In cases where using a MILP solver is undesirable (for example, if T_{\max} is very large and the MILP instances becomes a bottleneck), we propose an *incremental approach*. Here, we start with an arbitrary assignment of α values, which may or may not constitute an invariant, and iteratively change one α at a time. This change needs to be “in the right direction” — i.e., if our α ’s do not currently constitute an invariant, we need to weaken the bounds; and if they do constitute an invariant but that invariant is too weak to solve $\hat{\varphi}$, we need to tighten the bounds. The selection of which α to change and by how much to change it can be random, arbitrary, or according to some heuristic. In our experiments we observed that while this approach is computationally cheaper than solving MILP instances, it tends to lead to longer sequences of refining the α ’s before an appropriate invariant is found. Devising heuristics that will improve the efficiency of this approach remains a topic for future work.

4.4 Time-Dependent Properties

Our technique for verifying inferred invariants and for using them to solve the snapshot query (and hence to prove the property in question) hinges on our ability to reduce each step into an FFNN verification query. In order to facilitate this, we made the simplifying assumption that properties P and Q of the RNN verification query are time-agnostic; i.e. they are of the form $P = \bigwedge_{t=1}^{T_{\max}} \psi_1$ and $Q = \bigvee_{t=1}^{T_{\max}} \psi_2$ for ψ_1 and ψ_2 that are conjunctions of linear constraints. However, this limitation can be relaxed significantly.

Currently, input property P specifies a constant range for the inputs, e.g. $-3 \leq v_{1,1}^t \leq 3$ for all $1 \leq t \leq T_{\max}$. However, we observe that our technique can be applied also for input properties that encode linear time constraints; e.g. $4t \leq v_{1,1}^t \leq 5t$.

These properties can be transferred, as-is, to the FFNN snapshot network, and are compatible with our proposed technique. Likewise, the output property Q can also include constraints that are linear in t ; and can also restrict the query for a particular time step $t = t_0$. In fact, even more complex, piecewise-linear constraints can be encoded and are compatible with our technique. However, encoding these constraints might entail adding additional neurons to the RNN. For example, the constraint $(\max(v_{1,1}^t, v_{1,2}^t) \geq 5t)$ is piecewise-linear and can be encoded [6]; the encoding itself is technical, and is omitted to save space. As for constraints that are not piecewise-linear, if these can be soundly approximated using piecewise-linear constraints, then they can be soundly handled using our technique.

5 Evaluation

We created a proof-of-concept implementation of our approach as a Python module, called *RnnVerify*, which reads an RNN in TensorFlow format. The input and output properties, P and Q , and also T_{\max} , are supplied in a simple proprietary format, and the tool then automatically: (i) creates the FFNN snapshot network; (ii) infers a candidate invariant using the MILP heuristics from Section 4; (iii) formally verifies that I is an invariant; and (iv) uses I to show that $\hat{\varphi}$, and hence φ , are UNSAT. If $\hat{\varphi}$ is SAT, our module refines I and repeats the process. We intend to make our code publicly available with the final version of this paper.

For our evaluation, we focused on neural networks for *speaker recognition* — a task for which RNNs are commonly used, because audio signals tend to have temporal properties and varying lengths. We applied our verification technique to prove *adversarial robustness* properties of these networks, as we describe next.

Adversarial Robustness. It has been shown that *many* neural networks are susceptible to *adversarial inputs* [49]. These inputs are generated by slightly perturbing correctly-classified inputs, in a way that causes the misclassification of the perturbed inputs. Formally, given a network N that classifies inputs into labels l_1, \dots, l_k , an input x_0 , and a target label $l \neq N(x_0)$, an adversarial input is an input x such that $N(x) = l$ and $\|x - x_0\| \leq \delta$; i.e., input x is very close to x_0 , but is misclassified as label l . (There are additional, more complex variants of the problem [30]; we focus on this variant for simplicity.)

Adversarial robustness is a measure of how difficult it is to find an adversarial example — and specifically, what is the minimal amount of noise, i.e. the smallest δ , for which such an example exists. Verification can be used to find adversarial inputs or rule out their existence for a given δ , and consequently can find the smallest δ for which an adversarial input exists [6]. Using verification for proving the adversarial robustness of FFNNs has been studied extensively (e.g., [17,29,31,51]).

Speaker Recognition. A speaker recognition system receives a voice sample and needs to identify the speaker from a set of people. This is a private case of *speaker verification*, where a system needs to determine whether a voice sample belongs to a certain person. RNNs are often applied in implementing such systems [24], rendering them vulnerable to adversarial attacks [34]. Because such vulnerabilities in these systems pose a security concern [23], it is important to verify that their underlying RNNs afford high adversarial robustness.

Benchmarks. We trained 6 speaker recognition RNNs, based on the VCTK dataset [54]. Our networks are of modest, varying sizes: they each contain an input layer of dimension 40, one or two hidden layers with $d \in \{2, 4, 8\}$ memory units, followed by 1 to 3 fully connected, memoryless layers. The networks were trained to distinguish between 20 possible speakers.

Next, we selected 5 random, fixed input points $X = \{x_1, \dots, x_5\}$, that do not change over time; i.e. $x \in \mathbb{R}^{40}$ and $x_i^1 = x_i^2 = \dots$ for each $x_i \in X$. Then, for each RNN N and input $x_i \in X$, and for each value $2 \leq T_{\max} \leq 19$, we computed the ground-truth label $l = N(x_i)$, which is the label that received the highest score at time step T_{\max} . We also computed the label that received the second-highest score, l_{sh} , at time step T_{\max} . Then, for every combination of N , $x_i \in X$, and value of T_{\max} , we created the query

$$\underbrace{\langle \bigwedge_{t=1}^{T_{\max}} \|x'^t - x_i^t\|_{L_\infty} \leq 0.01, N, \underbrace{l_{sh} \geq l}_Q \rangle}_P$$

The allowed perturbation, at most 0.01 in L_∞ norm, was selected arbitrarily. The query is only **SAT** if there exists an input x' that is at distance at most 0.01 from x , but for which label l_{sh} is assigned a higher score than l at time step T_{\max} . This formulation resulted in a total of 540 benchmark queries. We then used RnnVerify to solve these queries, using an Intel i5 laptop with 8 cores and 8GB of memory.

We began by comparing our technique to the state of the art, namely unrolling [1]. We selected our smallest RNN — a network with only 2 memory units in one hidden layer, followed by a single fully connected layer. We compared the performance of unrolling to that of our tool, RnnVerify, for increasingly larger T_{\max} values. Both methods returned **UNSAT** results for all of these queries; however, the runtimes clearly demonstrate that our approach is far less sensitive to large T_{\max} values, and can perform orders-of-magnitude better than the state of the art when such values are encountered. Figure 7 summarizes the results.

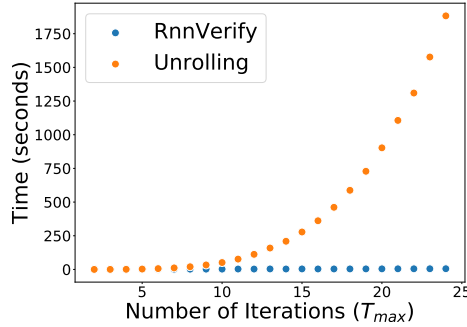


Fig. 7: Comparing the running time (in seconds) of RnnVerify and unrolling, as a function of T_{\max} . Both methods returned **UNSAT** on all queries.

Table 1 summarizes the performance of our approach over all 540 benchmark queries. We observe the following points (i) RnnVerify was usually able to decide

within a few seconds whether the inferred linear invariants could prove the desired property or not. The average run time over all 540 experiments was 2.67 seconds; (ii) we successfully proved that for 295 of the tested benchmarks, the RNN was robust around the tested point. For the remaining 245 benchmarks, our results are inconclusive: we do not know whether the network is vulnerable, or whether more sophisticated invariants are needed to prove robustness. Still, in the majority of tested benchmarks, the linear template proved useful; and (iii) we see that our linear invariants generally become less effective for larger values of T_{\max} . This is because the linear bounds become more loose as t increases, whereas the neurons' values typically do not increase significantly over time. This highlights the need for more expressive forms of invariants, perhaps to be combined with our current linear template.

Table 1: Running RnnVerify on our 540 benchmarks. Network $N_{x,y,z}$ has a hidden layer with x memory units; a second hidden layer with y memory units, if $y > 0$; and z fully connected layers. Each entry depicts the average runtime, in seconds, over the 5 input points; and also the number $x/5$ of queries where RnnVerify successfully proved adversarial robustness. In the remaining $5 - x$ queries, linear invariants were insufficient for proving that the snapshot query is **UNSAT**.

T_{\max}	$N_{2,0,1}$	$N_{2,0,2}$	$N_{4,0,2}$	$N_{4,0,3}$	$N_{4,2,3}$	$N_{8,0,2}$
2	1.27 (5/5)	1.38 (5/5)	1.32 (5/5)	1.37 (5/5)	2.78 (5/5)	1.96 (5/5)
3	1.32 (5/5)	2.15 (5/5)	1.34 (5/5)	1.58 (5/5)	5.47 (5/5)	2.63 (5/5)
4	1.51 (5/5)	1.49 (5/5)	1.60 (5/5)	1.56 (5/5)	2.31 (5/5)	1.88 (5/5)
5	1.86 (5/5)	1.51 (5/5)	1.63 (5/5)	72.23 (5/5)	3.02 (5/5)	1.57 (0/5)
6	1.49 (5/5)	1.63 (5/5)	1.55 (5/5)	1.76 (5/5)	2.93 (5/5)	1.76 (0/5)
7	2.58 (5/5)	1.70 (5/5)	1.69 (5/5)	3.39 (5/5)	2.87 (5/5)	2.04 (0/5)
8	1.49 (5/5)	1.79 (0/5)	1.60 (5/5)	1.63 (5/5)	1.93 (5/5)	2.27 (0/5)
9	1.42 (5/5)	1.65 (0/5)	1.60 (5/5)	1.60 (5/5)	2.24 (5/5)	2.10 (0/5)
10	1.47 (5/5)	1.72 (0/5)	4.62 (5/5)	1.71 (5/5)	2.04 (5/5)	1.97 (0/5)
11	1.45 (5/5)	1.74 (0/5)	1.64 (5/5)	1.81 (5/5)	2.44 (5/5)	2.28 (0/5)
12	1.26 (5/5)	1.71 (0/5)	1.36 (5/5)	1.35 (5/5)	3.76 (5/5)	1.70 (0/5)
13	1.14 (5/5)	1.56 (0/5)	1.43 (5/5)	1.30 (5/5)	2.59 (5/5)	1.78 (0/5)
14	1.23 (5/5)	3.06 (0/5)	2.34 (5/5)	1.54 (5/5)	2.30 (5/5)	1.77 (0/5)
15	3.15 (5/5)	1.39 (0/5)	1.23 (1/5)	3.57 (5/5)	2.91 (5/5)	1.99 (0/5)
16	1.25 (5/5)	1.66 (0/5)	1.40 (1/5)	1.34 (5/5)	2.72 (5/5)	2.29 (0/5)
17	1.30 (5/5)	1.49 (0/5)	1.41 (1/5)	1.34 (5/5)	3.09 (5/5)	1.97 (0/5)
18	1.34 (5/5)	1.78 (0/5)	1.42 (1/5)	2.00 (5/5)	3.21 (5/5)	2.22 (0/5)
19	1.38 (5/5)	4.12 (0/5)	3.89 (1/5)	1.56 (5/5)	2.88 (5/5)	5.83 (0/5)

6 Related Work

Due to the rise in neural network prevalence and the discovery of undesirable behaviors in many of them, the verification community has begun putting significant efforts into DNN verification. Recently proposed approaches include the use of SMT solving [27,29,31,36], LP and MILP solving [13,50], symbolic interval propagation [51], abstraction-refinement and abstract interpretation [14,17], and many

others (e.g., [5,12,18,21,32,39,41,48]). Our technique focuses on RNN verification, but uses an FFNN verification engine as a back-end. Consequently, it could be integrated with many of the aforementioned tools, and will benefit from any improvement in scalability of FFNN verification technology.

Whereas FFNN verification has received a great deal of attention, to the best of our knowledge only little research has been carried out on RNN verification. Akintunde et al. [1] were the first to propose such a technique, based on the notion of *unrolling* — the duplication of an RNN and concatenation of the copies, in order to create an equivalent FFNN. Ko et al. [33] proposed a similar framework, aimed at quantifying the robustness of an RNN to adversarial inputs — which can be regarded as an RNN verification technique tailored for a particular kind of properties. The scalability of both approaches is highly sensitive to the number of time steps, T_{\max} , specified by the property at hand.

The main advantage of our approach compared to the state of the art is that it is far less sensitive to the number of time steps being considered. Specifically, our construction of the snapshot query $\hat{\varphi}$ is oblivious to T_{\max} . This affords great potential for scalability, especially for long sequences of inputs. A drawback of our approach is that it requires invariant inference, which is known to be challenging.

Automated invariant inference is key in program analysis [43], especially for programs with loops, and has been studied extensively since the 70’s [10]. A few notable methods for doing so include: (i) abstract interpretation based: here, the program code is automatically analyzed in order to identify atoms from which an invariant formula can be constructed (e.g., [10,22,45]); (ii) counterexample-guided based: these approaches start with a candidate invariant generated, e.g., using program traces, and attempt to verify that it is truly an invariant. If the candidate fails, the counter-example returned by the verification tool is used to refine it (e.g., [3,42]); and (iii) learning based: recent work has suggested using machine learning to automatically suggest loop invariants [46]. It will be interesting to apply these techniques within the context of our framework, in order to more quickly and effectively discover useful invariants.

7 Conclusion

Neural network verification is an open problem that is becoming increasingly important to industry, regulators, and society as a whole. Research to date has focused primarily on FFNNs. We propose a novel approach for the verification of recurrent neural networks — a kind of neural networks that is particularly useful for context-dependent tasks, such as NLP. The cornerstone of our approach is the reduction of RNN verification to FFNN verification through the use of inductive invariants. Using a proof-of-concept implementation, we demonstrated that our approach can tackle many benchmarks orders-of-magnitude more efficiently than the state of the art. These experiments indicate the great potential that our approach holds.

Still, our work so far is but a first step, and we are already working on extending it along three axes. First, our approach depends greatly on our ability to generate useful inductive invariants to the problem at hand. Currently we have focused on invariants that adhere to linear templates; and we plan to experiment with additional approaches, such as those described in Section 6. Second, more work is

required to increase the scalability of our approach, especially for networks that contain multiple hidden layers with memory units. For such networks, generating sufficiently strong invariants is challenging, and we plan to tackle this difficult using *compositional verification* techniques in order to break the RNN into multiple, smaller networks, each with fewer memory units. Finally, the lack of available RNN verification benchmarks is a limiting factor; to mitigate it, we plan to apply our approach to additional, real-world RNN based systems.

Acknowledgements. This project was partially supported by grants from the Semiconductor Research Corporation, the Binational Science Foundation (2017662), the Israel Science Foundation (683/18), and the National Science Foundation (1814369).

References

1. M. Akintunde, A. Kevorchian, A. Lomuscio, and E. Pirovano. Verification of RNN-Based Neural Agent-Environment Systems. In *Proc. 33rd Conf. on Artificial Intelligence (AAAI)*, pages 6006–6013, 2019.
2. O. Bastani, Y. Ioannou, L. Lampropoulos, D. Vytiniotis, A. Nori, and A. Criminisi. Measuring Neural Net Robustness with Constraints. In *Proc. 30th Conf. on Neural Information Processing Systems (NIPS)*, 2016.
3. D. Beyer, T. Henzinger, R. Jhala, and R. Majumdar. The Software Model Checker BLAST. *Int. Journal on Software Tools for Technology Transfer (STTT)*, 9:505–525, 2007.
4. M. Bojarski, D. Del Testa, D. Dworakowski, B. Firner, B. Flepp, P. Goyal, L. Jackel, M. Monfort, U. Muller, J. Zhang, X. Zhang, J. Zhao, and K. Zieba. End to End Learning for Self-Driving Cars, 2016. Technical Report. <http://arxiv.org/abs/1604.07316>.
5. R. Bunel, I. Turkaslan, P. Torr, P. Kohli, and P. Mudigonda. A Unified View of Piecewise Linear Neural Network Verification. In *Proc. 32nd Conf. on Neural Information Processing Systems (NeurIPS)*, pages 4795–4804, 2018.
6. N. Carlini, G. Katz, C. Barrett, and D. Dill. Provably Minimally-Distorted Adversarial Examples, 2017. Technical Report. <https://arxiv.org/abs/1709.10207>.
7. K. Cho, B. van Merriënboer, Ç. Gülçehre, F. Bougares, H. Schwenk, and Y. Bengio. Learning Phrase Representations using RNN Encoder-Decoder for Statistical Machine Translation, 2014. Technical Report. <http://arxiv.org/abs/1406.1078>.
8. V. Chvátal. *Linear Programming*. W. H. Freeman and Company, 1983.
9. M. Cisse, Y. Adi, N. Neverova, and J. Keshet. Houdini: Fooling Deep Structured Visual and Speech Recognition Models with Adversarial Examples. In *Proc. 30th Advances in Neural Information Processing Systems (NIPS)*, pages 6977–6987, 2017.
10. P. Cousot and N. Halbwachs. Automatic Discovery of Linear Restraints Among Variables of a Program. In *Proc. 5th Symposium on Principles of Programming Languages (POPL)*, pages 84–96, 1978.
11. J. Devlin, M. Chang, K. Lee, and K. Toutanova. BERT: Pre-training of Deep Bidirectional Transformers for Language Understanding, 2018. Technical Report. <http://arxiv.org/abs/1810.04805>.
12. S. Dutta, S. Jha, S. Sanakaranarayanan, and A. Tiwari. Output Range Analysis for Deep Neural Networks. In *Proc. 10th NASA Formal Methods Symposium (NFM)*, pages 121–138, 2018.
13. R. Ehlers. Formal Verification of Piece-Wise Linear Feed-Forward Neural Networks. In *Proc. 15th Int. Symp. on Automated Technology for Verification and Analysis (ATVA)*, pages 269–286, 2017.

14. Y. Elboher, J. Gottschlich, and G. Katz. An Abstraction-Based Framework for Neural Network Verification. In *Proc. 32nd Int. Conf. on Computer Aided Verification (CAV)*, 2020.
15. J. Elman. Finding Structure in Time. *Cognitive Science*, pages 179–211, 1990.
16. R. Floyd. Assigning Meanings to Programs. In *Program Verification*, pages 65–81. Springer, 1993.
17. T. Gehr, M. Mirman, D. Drachsler-Cohen, E. Tsankov, S. Chaudhuri, and M. Vechev. AI2: Safety and Robustness Certification of Neural Networks with Abstract Interpretation. In *Proc. 39th IEEE Symposium on Security and Privacy (S&P)*, 2018.
18. S. Gokulanathan, A. Feldsher, A. Malca, C. Barrett, and G. Katz. Simplifying Neural Networks with the Marabou Verification Engine. In *Proc. 12th NASA Formal Methods Symposium (NFM)*, 2020.
19. I. Goodfellow, Y. Bengio, and A. Courville. *Deep Learning*. MIT Press, 2016.
20. I. Goodfellow, J. Pouget-Abadie, M. Mirza, B. Xu, D. Warde-Farley, S. Ozair, A. Courville, and Y. Bengio. Generative Adversarial Nets. In *Proc. 27th Advances in Neural Information Processing Systems (NIPS)*, pages 2672–2680, 2014.
21. D. Gopinath, G. Katz, C. Păsăreanu, and C. Barrett. DeepSafe: A Data-driven Approach for Checking Adversarial Robustness in Neural Networks. In *Proc. 16th. Int. Symp. on Automated Technology for Verification and Analysis (ATVA)*, pages 3–19, 2018.
22. S. Gulwani and N. Jojic. Program Verification as Probabilistic Inference. In *Proc. 34th Symposium on Principles of Programming Languages (POPL)*, pages 277–289, 2007.
23. A. Hadid, N. Evans, S. Marcel, and J. Fierrez. Biometrics systems under spoofing attack: an evaluation methodology and lessons learned. *IEEE Signal Processing Magazine*, 32(5):20–30, 2015.
24. G. Heigold, I. Moreno, S. Bengio, and N. Shazeer. End-to-end Text-Dependent Speaker Verification. In *2016 IEEE International Conference on Acoustics, Speech and Signal Processing, ICASSP*, pages 5115–5119, 2016.
25. G. Hinton, L. Deng, D. Yu, G. Dahl, A. Mohamed, N. Jaitly, A. Senior, V. Vanhoucke, P. Nguyen, T. Sainath, and B. Kingsbury. Deep Neural Networks for Acoustic Modeling in Speech Recognition: The Shared Views of Four Research Groups. *IEEE Signal Processing Magazine*, 29(6):82–97, 2012.
26. S. Hochreiter and J. Schmidhuber. Long Short-term Memory. *Neural Computation*, pages 1735–1780, 1997.
27. X. Huang, M. Kwiatkowska, S. Wang, and M. Wu. Safety Verification of Deep Neural Networks. In *Proc. 29th Int. Conf. on Computer Aided Verification (CAV)*, pages 3–29, 2017.
28. K. Julian, J. Lopez, J. Brush, M. Owen, and M. Kochenderfer. Policy Compression for Aircraft Collision Avoidance Systems. In *Proc. 35th Digital Avionics Systems Conf. (DASC)*, pages 1–10, 2016.
29. G. Katz, C. Barrett, D. Dill, K. Julian, and M. Kochenderfer. Reluplex: An Efficient SMT Solver for Verifying Deep Neural Networks. In *Proc. 29th Int. Conf. on Computer Aided Verification (CAV)*, pages 97–117, 2017.
30. G. Katz, C. Barrett, D. Dill, K. Julian, and M. Kochenderfer. Towards Proving the Adversarial Robustness of Deep Neural Networks. In *Proc. 1st Workshop on Formal Verification of Autonomous Vehicles, (FVAV)*, pages 19–26, 2017.
31. G. Katz, D. Huang, D. Ibeling, K. Julian, C. Lazarus, R. Lim, P. Shah, S. Thakoor, H. Wu, A. Zeljić, D. Dill, M. Kochenderfer, and C. Barrett. The Marabou Framework for Verification and Analysis of Deep Neural Networks. In *Proc. 31st Int. Conf. on Computer Aided Verification (CAV)*, pages 443–452, 2019.

32. Y. Kazak, C. Barrett, G. Katz, and M. Schapira. Verifying Deep-RL-Driven Systems. In *Proc. 1st ACM SIGCOMM Workshop on Network Meets AI & ML (NetAI)*, pages 83–89, 2019.
33. C. Ko, Z. Lyu, T. Weng, L. Daniel, N. Wong, and D. Lin. POPQORN: Quantifying Robustness of Recurrent Neural Networks. In *Proc. 36th IEEE Int. Conf. on Machine Learning and Applications (ICML)*, 2019.
34. F. Kreuk, Y. Adi, M. Cisse, and J. Keshet. Fooling End-to-End Speaker Verification with Adversarial Examples. In *Proc. IEEE Int. Conf. on Acoustics, Speech and Signal Processing (ICASSP)*, pages 1962–1966, 2018.
35. A. Krizhevsky, I. Sutskever, and G. Hinton. Imagenet Classification with Deep Convolutional Neural Networks. In *Proc. 25th Advances in Neural Information Processing Systems (NIPS)*, pages 1097–1105, 2012.
36. L. Kuper, G. Katz, J. Gottschlich, K. Julian, C. Barrett, and M. Kochenderfer. Toward Scalable Verification for Safety-Critical Deep Networks, 2018. Technical Report. <https://arxiv.org/abs/1801.05950>.
37. G. Lample and D. Chaplot. Playing FPS Games with Deep Reinforcement Learning. In *Proc. 31st Conference on Artificial Intelligence (AAAI)*, pages 2140–2146, 2017.
38. Z. Lipton, D. Kale, C. Elkan, and R. Wetzell. Learning to Diagnose with LSTM Recurrent Neural Networks. In *Proc. 4th Int. Conf. on Learning Representations (ICLR)*, 2016.
39. A. Lomuscio and L. Maganti. An Approach to Reachability Analysis for Feed-Forward ReLU Neural Networks, 2017. Technical Report. <http://arxiv.org/abs/1706.07351>.
40. R. Nallapati, B. Xiang, and B. Zhou. Sequence-to-Sequence RNNs for Text Summarization, 2016. Technical Report. <http://arxiv.org/abs/1602.06023>.
41. N. Narodytska, S. Kasiviswanathan, L. Ryzhyk, M. Sagiv, and T. Walsh. Verifying Properties of Binarized Deep Neural Networks, 2017. Technical Report. <http://arxiv.org/abs/1709.06662>.
42. T. Nguyen, T. Antonopoulos, A. Ruef, and M. Hicks. Counterexample-Guided Approach to Finding Numerical Invariants. In *Proc. 11th Joint Meeting on Foundations of Software Engineering (FSE)*, pages 605–615, 2017.
43. F. Nielson, H. Nielson, and C. Hankin. *Principles of Program Analysis*. Springer, 1999.
44. O. Padon, N. Immerman, S. Shoham, A. Karbyshev, and M. Sagiv. Decidability of Inferring Inductive Invariants. In *Proc. 43th Symposium on Principles of Programming Languages (POPL)*, pages 217–231, 2016.
45. R. Sharma, I. Dillig, T. Dillig, and A. Aiken. Simplifying Loop Invariant Generation Using Splitter Predicates. In *Proc. 23rd Int. Conf. on Computer Aided Verification (CAV)*, pages 703–719, 2011.
46. X. Si, H. Dai, M. Raghothaman, M. Naik, and L. Song. Learning Loop Invariants for Program Verification. In *Proc. 32nd Conf. on Neural Information Processing Systems (NeurIPS)*, pages 7762–7773, 2018.
47. D. Silver, A. Huang, C. Maddison, A. Guez, L. Sifre, G. Van Den Driessche, J. Schrittwieser, I. Antonoglou, V. Panneershelvam, M. Lanctot, and S. Dieleman. Mastering the Game of Go with Deep Neural Networks and Tree Search. *Nature*, 529(7587):484–489, 2016.
48. G. Singh, T. Gehr, M. Püschel, and M. Vechev. An Abstract Domain for Certifying Neural Networks. In *Proc. 46th Symposium on Principles of Programming Languages (POPL)*, 2019.
49. C. Szegedy, W. Zaremba, I. Sutskever, J. Bruna, D. Erhan, I. Goodfellow, and R. Fergus. Intriguing Properties of Neural Networks, 2013. Technical Report. <http://arxiv.org/abs/1312.6199>.

50. V. Tjeng, K. Xiao, and R. Tedrake. Evaluating Robustness of Neural Networks with Mixed Integer Programming. In *Proc. 7th Int. Conf. on Learning Representations (ICLR)*, 2019.
51. S. Wang, K. Pei, J. Whitehouse, J. Yang, and S. Jana. Formal Security Analysis of Neural Networks using Symbolic Intervals. In *Proc. 27th USENIX Security Symposium*, pages 1599–1614, 2018.
52. P. Werbos. Generalization of Backpropagation with Application to a Recurrent Gas Market Model. *Neural Networks*, pages 339–356, 1988.
53. W. Xiang and T. Johnson. Reachability Analysis and Safety Verification for Neural Network Control Systems, 2018. Technical Report. <http://arxiv.org/abs/1805.09944>.
54. J. Yamagishi, C. Veaux, and K. MacDonald. CSTR VCTK Corpus: English Multi-speaker Corpus for CSTR Voice Cloning Toolkit, 2019. University of Edinburgh. <https://doi.org/10.7488/ds/2645>.